PAPER

Aerobic Intramolecular Carbon-Hydrogen Bond Oxidation Promoted by Cu(I) Complexes

Received 00th January 20xx,
Accepted 00th January 20xx

DOI: 10.1039/x0xx00000x

María Álvarez,[a] Francisco Molina,[a] Manuel R. Fructos,[a] Juan Urbano,[b] Eleuterio Álvarez,[c] Mariona Sodupe,[d] Agustí Lledós,*[d] and Pedro J. Pérez*[a]

The oxidation of C-H bonds by copper centres at enzymes with molecular oxygen takes place in nature at ambient conditions. Herein we report a similar transformation in which under ambient pressure and temperature (1 atm, 25 °C) the complex $Tp^{Ms}Cu(THF)$ (Tp^{Ms} = hydrotris(3-mesityl-pyrazol-1-yl)borate) undergoes the intramolecular oxidation of an alkylic C-H bond with O_2, leading to the formation of a trinuclear compound where alkoxy and hydroxyl ligands are bonded to the copper centres, as inferred from X-ray studies. The presence of adventitious Cu(0) derived from partial decomposition of the initial $Tp^{Ms}Cu(THF)$ facilitates the formation of such trinuclear compound. DFT studies support the reaction taking place through a Cu(III) alkoxy-hydroxyl copper intermediate.

Introduction

Copper enzymes are ubiquitous in Nature, mainly involved in oxidation processes with O_2 as the oxygen source.[1] In the context of carbon-hydrogen bond oxidations, oxygenases are responsible for the hydroxylation of highly inert hydrocarbons,[2] as it is the case of methane monooxygenases (MMOs), responsible for the conversion of methane into methanol in methanotrophic bacteria.[3] Particulate MMO is a copper-containing enzyme for which the nuclearity of the active site involved in O_2 activation has been the subject of controversy for the last decade. A very recent report has concluded[4] that despite the closeness of two copper units, it is a monocopper site the one that is able to catalyse methane oxidation. From this perspective, work carried out in the last decades with mononuclear copper complexes toward O_2 activation regain more interest,[5] particularly in the context of subsequent C-H bond oxidations. Outstanding advances in this area such as the intramolecular oxidation (Scheme 1) of C_{sp3}-H bonds of the ancillary ligand (usually a bis-, tris- or tetracoordinated, N-donor ligand) as a model for biological systems have been achieved.[6] These transformations occur through the generation of end-on copper(II)-superoxide complexes $LCu^{II}(O_2\bullet)$,[7] some of them being detected or isolated, from the reaction of a Cu(I) complex with O_2, which can take place within several pathways.[8,9,10,11,12]

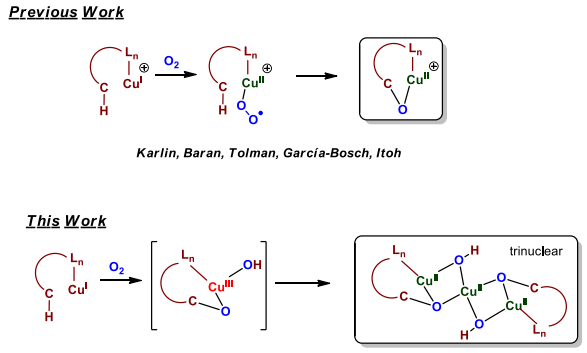

Scheme 1 The intramolecular C-H bond oxidation with Cu(I) complexes.

In view of the importance of these studies relative to the development of biomimetic catalytic systems, we have focused in the aerobic oxidation of the complex $Tp^{Ms}Cu(THF)$ (**1-THF**) (Tp^{Ms} = hydrotris(3-mesityl-pyrazol-1-yl)borate) and found that the hydroxylation of a C_{sp3} bond of the mesityl fragment takes place under very mild conditions. DFT studies and experimental evidences allow proposing the implication of a Cu(II)-Cu(I) dinuclear intermediate.

[a] Laboratorio de Catálisis Homogénea, Unidad Asociada al CSIC CIQSO-Centro de Investigación en Química Sostenible and Departamento de Química, Universidad de Huelva, 21007-Huelva (Spain).
[b] Departamento de Química, Universidad de Huelva, 21007-Huelva (Spain).
[c] Instituto de Investigaciones Químicas, Centro de Investigaciones Isla de la Cartuja, Avda Américo Vespucio 49,41092 Sevilla (Spain)
[d] Departament de Química, Universitat Autònoma de Barcelona, 08193 Cerdanyola del Vallès, Barcelona (Spain).
E-mail: agusti@klingon.uab.es.

† Electronic Supplementary Information (ESI) available: All procedures and characterization data for new compounds, additional computational data and Cartesian coordinates and energies of the optimized structures. See DOI:10.1039/x0xx00000x

Results and Discussion

Reaction of Tp^{x}Cu cores with molecular dioxygen

We first investigated the reaction of Tolman's complex Tp^{Ms}Cu(THF)[13] (**1-THF**) with O_2 in tetrahydrofuran at room temperature. When this complex was dissolved in an O_2-saturated solvent, the initially colourless solution smoothly became greenish with time, leading to the formation of green crystals within 24h at that temperature. The formation of this crystalline material result is independent of the solvent, since acetone, toluene or dichloromethane solutions led to the same outcome, albeit at variable time. The product was completely insoluble in organic solvents, precluding the use of NMR techniques. The IR spectra showed an absorption centered at 3652 cm^{-1}, in the typical region for ν(O-H). Elemental analysis was consistent with the formulation $(Tp^{Ms})_2(O_2)_2Cu_3$, indicating a significant deviation from the initial 1:1 Tp^{Ms}:Cu stoichiometry. Fortunately, the crystalline material formed, in all the above solvents, was suitable for X-ray studies,[14] allowing the determination of the solid structure of the molecules of this new complex **2a**. It contains three copper centres with two different environments (Scheme 2). On one hand, the central copper Cu_C is connected to four oxygen donors, in a square-planar fashion. On the other, the lateral copper Cu_L ions are five coordinate, bonded to the three N donors of the Tp^{Ms} ligand, in a κ^3 mode, as well as to two oxygen donors, shared with Cu_C, in a square-pyramidal environment. One of the oxygen atoms corresponds to a hydroxyl group (which generate that band in the IR spectrum) and the other one to an alkoxy group derived from the oxidation of one of the C_{sp3}-H bonds of the mesityl ring in the ancillary ligand. The reaction has been carried out up to a scale of 0.35 g (0.05 mmol) of **1-THF**, leading to the isolation of 0.158 g of **2a**.(1.1 x 10^{-4} mmol). Assuming that molecules of **1a** are required for the formation of **2a**, the isolated yield is 68%.

Ligand hydroxylation with copper complexes leading to alkoxy (or aryloxy)-hydroxy derivatives is a well-known process for dinuclear compounds. Seminal work by Karlin[15] in 1982 showed the oxidation of an aryl C-H bond and the formation of a hydroxyl ligand, and several related examples were further reported.[16] These transformations occurs through the activation of the dioxygen molecule by a Cu_2 core, at variance with our system, which cannot accommodate an O_2 molecule between two Tp^{Ms}Cu units due to the steric hindrance of the Ms substituents (see below), thus occurring by a mononuclear O_2 activation, similar to that reported by Kitajima and Solomon,[7a,b]

The structure of complex **2a** is similar to that reported by Pierpont for [Cu{Tp^{Cum,Me}Cu(μ-OMe)$_2$}$_2$][17] albeit using a rather distinct synthesis route, excluding O_2/C-H bond activation processes. Two of the Cu_L-N_{pyr} distances are very close (2.013(4) and 2.026(4) Å) whereas the third one is significantly longer (2.369(4) Å). The Cu_L– Cu_C distances of 3.007(7) Å surpasses that of the sum of van der Waals radii[18] for two Cu (2.40 Å), discarding any Cu-Cu bonding interaction. It is also worth mentioning that the measurement of the magnetic moment μ_{eff} (Evans balance, see SI) led to a value of 3.3 MB, which is close to that expected for three unpaired electrons. This is at variance with the above complexes described by Pierpont,[17] which displayed μ_{eff} = 1.82 MB, but similar to the trinuclear copper complex [Cu$_3$(m-methoxybenzoato)$_4$(H$_2$TEA)$_2$][19] (TEA = triethanolaniline) described by Ferreti, also containing two O-bridges between each couple of Cu ions, and with μ_{eff} = 3.4 MB.

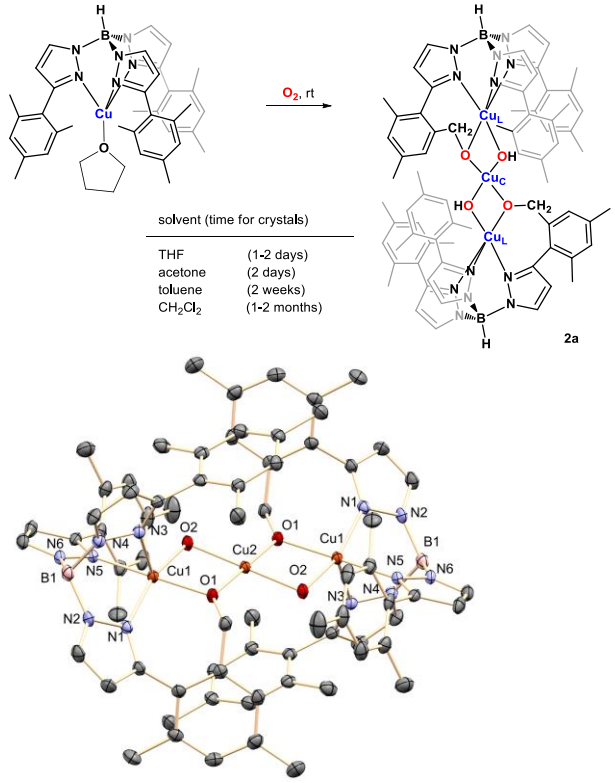

Scheme 2 The trinuclear complex **2a** and its molecular structure (H atoms omitted for clarity).

The formation of **2a** from Tp^{Ms}Cu(THF) and O_2 requires partial decomposition of the initial copper complex at some extent to provide the third copper centre. Since ligand degradation can proceed at the B-H group,[20] we also prepared the boron-substituted MeTp^{Ms} ligand,[21] for which the corresponding Me-Tp^{Ms}Cu(THF) complex could not be isolated. Thus, we synthetized the new complexes Tp^{Ms}Cu(NCPh) (**1a**) and Me- Tp^{Ms}Cu(NCPh) (**1b**), only differing in the substitution at boron. When these complexes were submitted to the conditions which provided **2a** from **1-THF**, green crystalline materials were isolated in both cases, corresponding to the trinuclear complexes **2a** and **2b** (Scheme 3). The latter has also been characterized by X-ray studies (see ESI for X-ray characterization).[14] It is worth noting the different in the yields observed: 2a was isolated in 71% yield, showing that the THF or nitrile ligands in the starting materials do not influence the reaction, whereas 2b was separated in only 25% yield (0.2 g reaction scale)

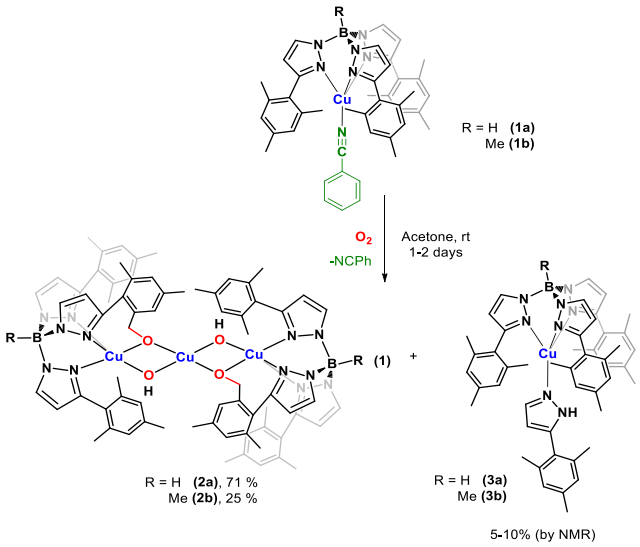

Scheme 3 Synthesis of the complexes **2a** and **2b** from nitrile adducts **1a,b**).

NMR monitoring of the consumption of **1a** only showed the disappearance of its resonances, as well as the formation of minor amounts (ca. 5-10%) of the new complex $Tp^{Ms}Cu(Hpyr^{Ms})$ (**3a**, $Hpyr^{Ms}$ = 3-mesitylpyrazole), demonstrating the availability of free pyrazole from partial degradation of the initial copper complex. This compound has been independently synthetized and characterized, including X-ray studies (see SI).[14] Since the only difference between both reactants **1a** and **1b**[14] is the group attached at boron (H or Me), we believe that the observed distinct reactivity must be related to the different reducing power of both moieties,[22] which must be responsible of the partial decomposition of the starting Cu(I) complexes including the trapped free pyrazole. It is worth mentioning that at variance with other systems, where H_2O_2 is proposed to form from O_2 activation,[9c] en route to the copper hydroperoxide, in our case the reaction of $Tp^{Ms}Cu(L)$ (L = THF, NCPh) with H_2O_2 does not induce the formation of **2a**.

Since two $Tp^{Ms}Cu$ units and a third "naked" Cu ion form the trinuclear compounds, we reasoned that the latter could come from some metallic copper formed from the partial decomposition of the starting materials. Thus, we carried out twin experiments with $Tp^{Ms}Cu(L)$ (L = THF or NCPh) and O_2 in THF or acetone, in the absence or presence of added metallic copper. The results were the same in all cases: those experiments having added metallic copper showed the formation of **2a** at a higher rate, which could be visually observed (Figure 1.1). Unfortunately, the exact yields could not be calculated since excess of metallic copper could not be completely separated from crystalline material. In any case, we believe that these experiments demonstrate the involvement of metallic copper in the formation of the trinuclear complex **2a**.

Monitoring of the reaction by UV-Vis has provided valuable information. Fig. 1 shows the variation with time of such spectra for the experiments carried out with and without added metallic copper, under the same conditions of initial Cu(I) concentration (0.035 M) and at room temperature (no reaction is observed at temperatures lower than 0 °C). A band centred at ca. 675 nm increases with time until 24 h, then decreasing when microcrystalline material of **2a** comes out of the solution. We assume from this observation that this band corresponds to **2a**, consistently with the low absorbance values. Since solutions of isolated **2a** were not available due to its insolubility in most organic solvents, TD-DFT calculations were performed to confirm that assignment. Only the

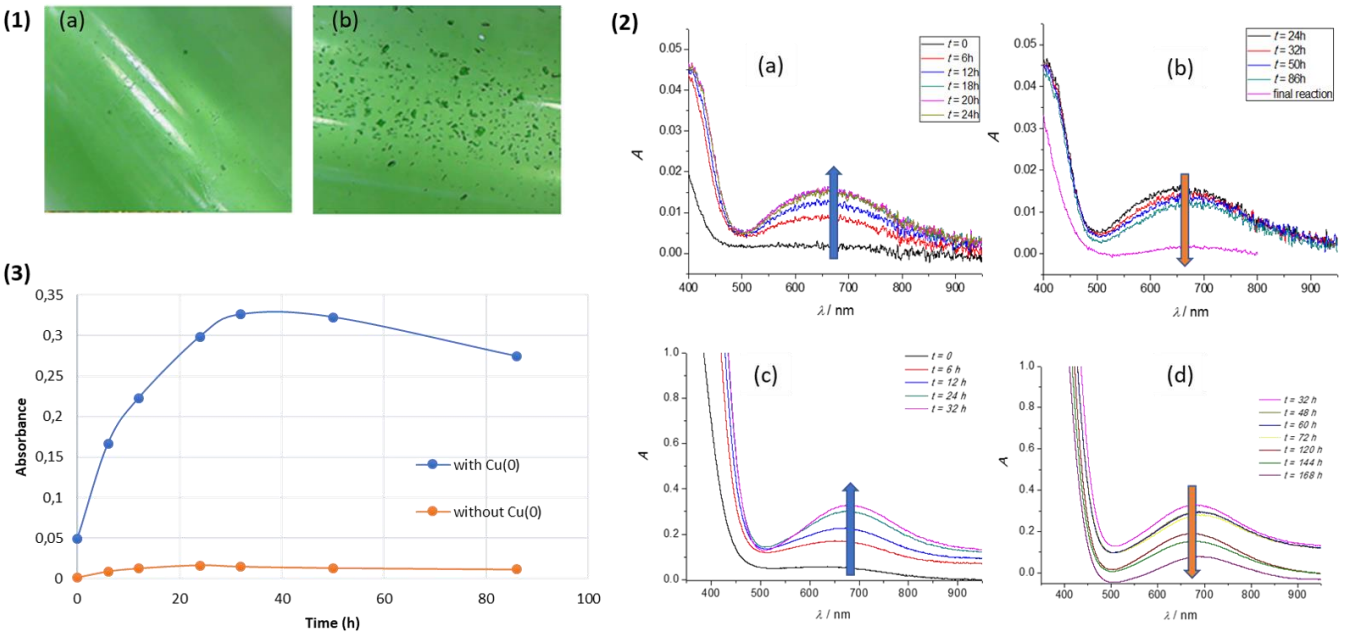

Fig. 1 (1)(a) Formation of **2a** from $Tp^{Ms}Cu(THF)$ and O_2 at room temperature after 12 h. (b) Same experiment in the presence of metallic copper (Cu(0) powder) added. (2) UV-Vis monitoring of the reaction of complex $Tp^{Ms}Cu(THF)$ (0.025 M) and O_2 at room temperature (a,b): no metallic copper (Cu(0)) added. (c,d) metallic copper (Cu(0)) added. (3) Comparison for absorbance values at 675 nm

.

trimetallic complex (and not mononuclear or dinuclear ones) displays the most intense band in this region. In particular, the simulated spectrum (see ESI) shows a band at ca. 620 nm that corresponds to Cu d → Cu d transitions. A similar behaviour was found for the experiment containing added metallic copper, albeit the absorbance increased with a twenty-fold factor (maximum of ca. 0.3 vs 0.015, see Fig. 1), We interpret this observation as a proof of the need of metallic copper for the formation of **2a**.

Reactivity of Tp^{x}Cu(I) complexes with O_2: mechanistic aspects

Trinuclear complexes **2a** and **2b** contain two oxygen atoms bonded to the lateral copper centres, which could correspond to the initial O_2 molecule, albeit we have no experimental evidence to support it. On the other hand, experimental evidences point out the key role of Cu(0) in their formation, although no intermediate along the reaction pathway from **1-THF** to **2a** has been isolated. On these bases, DFT calculations have been performed to provide additional information toward the understanding of this transformation and to identify potential intermediates (see ESI for calculations details).

Mechanistic considerations

From Itoh's work[12] and our experimental evidences, a plausible reaction pathway, depicted in Scheme 4, can be proposed. Initially, a Tp^{Ms}Cu^{II}(O_2•) superoxide (**A**) would form from Tp^{Ms}Cu^{I}(THF) and O_2, which could be either end-on or side-on. Subsequent hydrogen atom abstraction process (HAT) takes place generating a hydroperoxide and a carbon-centred radical at the alkyl substituent of the mesityl ring (**B**). From this intermediate, the O-O cleavage would lead to the formation of C-O and Cu-O bonds in intermediate **C**, which could be either a Cu(II) or Cu(III) species, both bearing alkoxy and hydroxyl ligands bonded to the metal centre. Interestingly, this intermediate could evolve toward a Cu-oxyl and hydroxyl radical, and/or originate Fenton chemistry as proposed by Karlin and others.[9b] However this does not seem to be the case since at this stage Cu(0), either adventitious by partial decomposition of the starting material or externally added, would promote the reduction of two units of such intermediate leading to the formation of **2a**. DFT calculations will give the complete energy landscape of the reaction and identify the key intermediates.

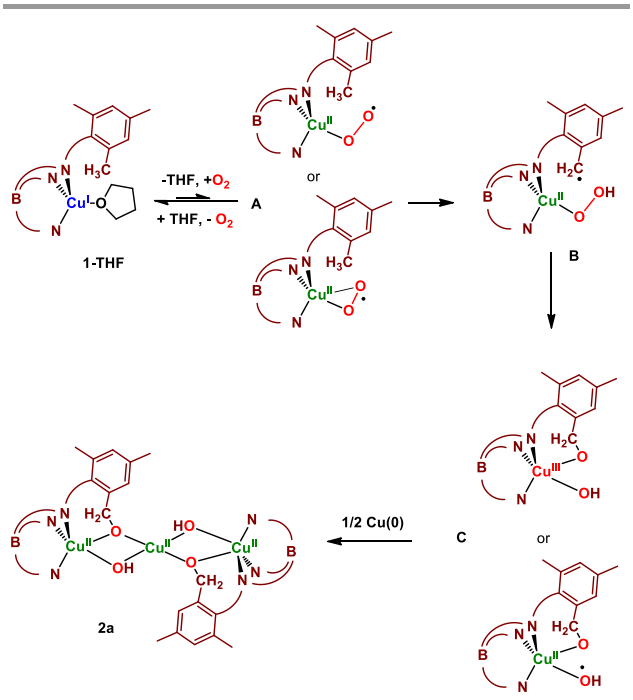

Scheme 4 Plausible reaction pathway toward the formation of complex **2a**.

*From **1-THF** to intermediate **C**: C-H bond oxidation.*

Tp^{Ms}Cu^{I}(THF) (**1**-THF) can easily dissociate the THF ligand (ΔG_{THF} = 14.0 kcal mol^{-1}) to generate species **1** that will coordinate the O_2 molecule in **1-O$_2$**. The hydroxylation reaction that leads to **C** starts with a Cu(I) complex with a singlet spin state and a O_2 molecule with a triplet spin state. We have only considered mononuclear copper species along the reaction pathway, discarding dinuclear species. It is evident from the optimized structure of **1** (Fig. 2, top) that the mesityl wings in the Tp^{Ms} ligand preclude the formation of such species. Attempts to stabilize by DFT calculations a Tp$^{Ms}_2$Cu$_2$ unit were unsuccessful. This is in agreement with the previous observation of mononuclear O_2 activation by bulky Tp^{x}Cu cores.[7a,b]

Three different electronic scenarios have been considered for this reaction: triplet (T), open-shell singlet (OSS) and closed-shell single (CSS). Fig. 3 depicts the Gibbs energy profile in THF for the most favourable pathway for the reaction (triplet state). Transition state structures connecting the different species of this profile are gathered in Fig. 4. The exploration of the potential energy surface (PES) has been performed with the TPSSh functional, including dispersion corrections (TPSSh-D3), with a SMD continuum description of the THF solvent (see ESI). Gibbs energy profiles for the open- and closed-shell singlet energy surfaces explored can be found at the ESI. It must be pointed out that most of the intermediates and transition states have very similar geometries and energies in

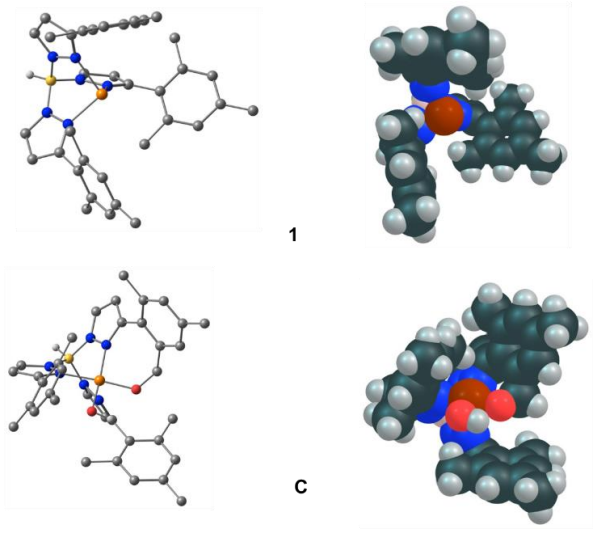

Fig. 2 Optimized structures of the Tp^{Ms}Cu core (**1**) and intermediate C in Scheme 4 (left) and their space filling pictures (right). C-H bonded hydrogen atoms have been omitted in the optimized geometries.

the T and OSS potential energy surfaces.

Coordination of O_2 to the $Tp^{Ms}Cu$ core (**1**) yields the copper(II) side-on superoxo complex **1-O₂**, which lies 4.8 kcal mol^{-1} below the separated reactants (Fig. 3). Triplet is the ground state of **1-O₂**, the ope(CO)n-shell-singlet and closed-shell-singlet structures lying 10.0 and 12.7 kcal mol^{-1} above the triplet complex, respectively. It should be noted that all attempts to characterize an end-on isomer in our system reverted to the side-on conformation, at variance to Itoh's system, bearing a different N-tridentate ligand (N-[2-"2-pyridyl)ethyl]-1,5-diazacyclooctane), for which calculations[12] found the existence of two Cu(II)-superoxide isomers, end-on and side-on, with very similar energies (end-on 0.6 kcal mol^{-1} more stable than side-on). Furthermore, side-on coordination of the superoxo ligand were disclosed independently by Kitajima and Solomon, including X-ray analysis, in copper-superoxo complexes bearing highly hindered hydrotris(pyrazolyl)borate ligands.[7a,b] Those ligands contained bulky alkyl groups at the pyrazolyl rings (tBu, iPr, Ad), at variance with the aromatic rings in 1a,b. Previous studies from our laboratory showed[23] significant differences in the redox properties of the copper centre derived from such those substitutions. For example, the E_{pa} (mv) of $Tp^{Cy}Cu(CO)$ (Cy, cyclohexyl) was recorded as 515 whereas that of $Tp^{Ms}Cu(CO)$ was 603. A difference in the ν(CO) was also found: 2064 and 2079 for Tp^{Cy} and Tp^{Ms}, respectively. We believe that these electronic differences may affect the nature of the spin and the reactivity.

for our system (25.5 kcal mol^{-1}) compared to the Itoh's one (21.8 kcal mol^{-1}) could be related with the stronger C-H bond in our system (methyl vs. benzyl C-H bonds).[24]

In **I-OOH** the unpaired electron at the organic moiety is spread over the carbon atom that has transferred the hydrogen and the two oxygen atoms. The O-O distance has notably elongated in the hydroperoxo ligand (from 1.31 Å in **1-O₂** to 1.46 Å in **1-OOH**) favouring the splitting into the O and OH fragments. At this point the reaction can follow two different pathways (A and B, Fig. 3) depending on which one of the two fragments binds to the copper and carbon centres. In pathway A after the O-OH bond breaking (**TS$_{CO}$**, Fig. 4) the OH group binds the copper centre and the O atom binds the radical carbon centre. In this way the O-OH scission leads directly to the final product **C**. However, before the O-O scission the OOH group must rotate (**TS$_{rot}$**) to achieve the right conformation for the rupture to take place. In pathway B the CH_2 group is hydroxylated and a copper(II) oxyl is formed (**I-COH**). Abstraction of the hydrogen atom of the hydroxyl group by the copper(II) oxyl group (**TS$_{OHO}$**) generates the same intermediate **C** than pathway A. In both pathways the highest point in the energy profile corresponds to the O-OH bond breaking step (Fig. 3). However, the transition state in pathway A (**TS$_{CO}$**) is 4.5 kcal mol^{-1} lower than that in pathway B (**TS$_{COH}$**), pointing out that pathway A is favoured, as found for the Itoh's system.[10c] Very similar results are obtained for the reaction in the open-shell singlet state; i.e., **TS$_{CO}$-OSS** is found at 24.1 kcal mol^{-1}, 4.7

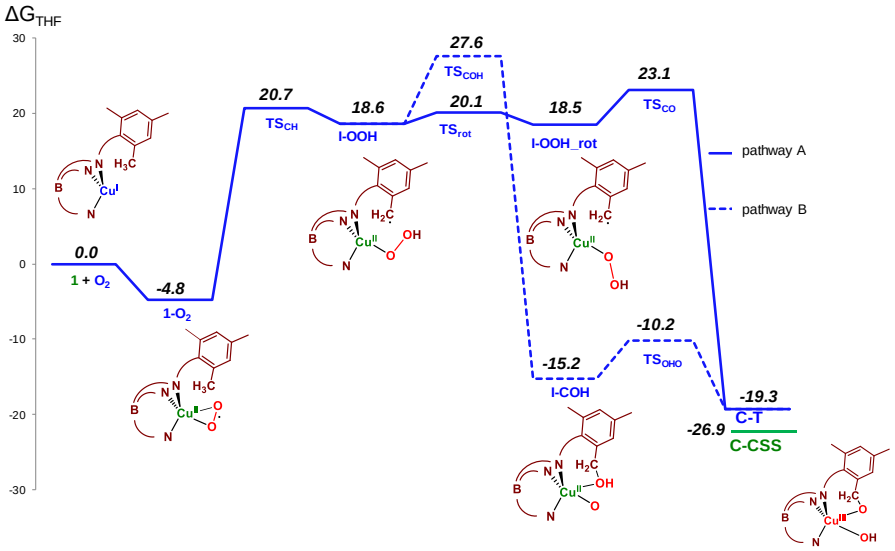

Fig. 3 DFT-computed (TPSSh-D3/BS2) Gibbs energy profile for the reaction of **1** with O_2 in tetrahydrofuran in the triplet state. Relative ΔG values are given in kcal mol^{-1} and are reported with respect to separated **1** and O_2.

The **1-O₂** complex has one unpaired electron at the copper centre and another one distributed between the two oxygen atoms of the superoxide unit and is capable to abstract a hydrogen atom from the closest methyl substituent of one mesityl ring in the next step. The hydrogen atom abstraction takes places through the transition state **TS$_{CH}$** with a barrier of 25.5 kcal mol^{-1} and leads to the copper(II) hydroperoxo intermediate **I-OOH**. The somewhat higher calculated barrier kcal mol^{-1} below **TS$_{COH}$-OSS** (28.8 kcal mol^{-1}). Noticeably, the reaction in the closed-shell singlet state features a significantly higher barrier (34.1 kcal mol^{-1}), which corresponds to the abstraction of a C-H proton by the peroxo ligand (**TS$_{CH}$-CSS**), entailing the concomitant O-O bond breaking and formation of copper-oxo and alcohol groups (see Supporting Information). Optimization of the hydroperoxide intermediate **I-OOH** in the closed-shell singlet state, starting from the triplet geometry, gives intermediate **I-COH-CSS** with a copper(III)-oxo/C-OH

nature, at 1.9 kcal mol^{-1}. We have explored this alternative route to enter into the Cu(III) region, by locating the crossing point (minimum energy crossing point, MECP) between the triplet and singlet surfaces that connects both intermediates. This MECP is found at 31.0 kcal mol^{-1}, much higher than **TS$_{rot}$** and **TS$_{CO}$** in the triplet surface. Therefore, this alternative route to reach **C** can be discarded.

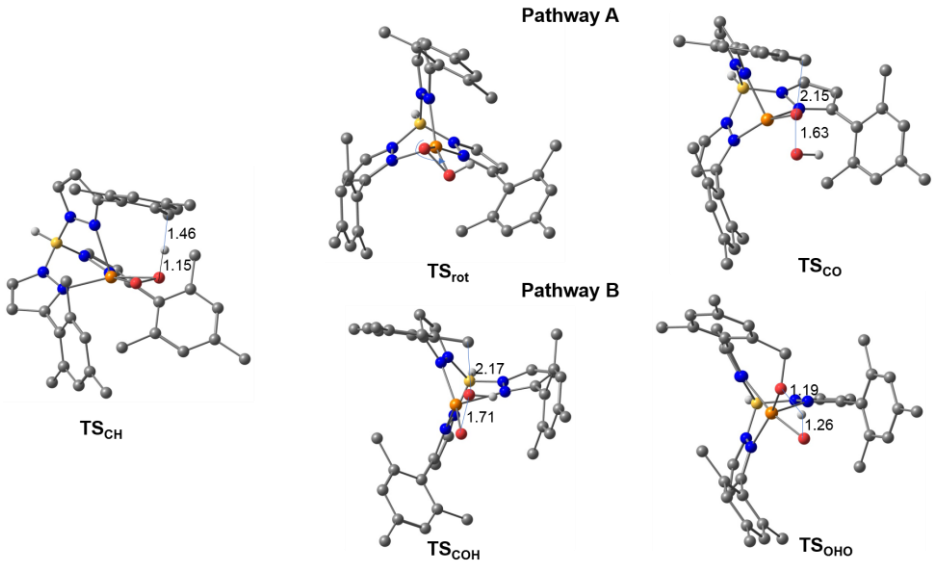

Fig. 4 Optimized geometries of the transition states in the Gibbs energy profile of Fig. 3. Distances in Å.

As a conclusion of this mechanistic investigation, pathway A in the triplet PES appears as a feasible mechanism for the formation of the mononuclear alkoxy-hydroxyl intermediate **C**.

*Nature of intermediate **C**: A Cu(II) or Cu(III) centre?*

In the triplet state, intermediate **C** can be described as a Cu(II) centre with an additional unpaired electron delocalized over the two oxygen atoms. An alternative description of this intermediate is obtained in the closed-shell singlet state: a formally Cu(III) centre with an hydroxyl ligand. Optimization of **C** in the CSS state gives a structure notably more stable than the triplet (**C-CSS**, 7.6 kcal mol^{-1} below **C-T**). Indeed, in the OSS PES **TS$_{OHO}$** leads directly to this structure. The structural features of the singlet and triplet isomers of **C** are similar. The main difference is found in the Cu-N distance with the nitrogen atom above the plane defined by the two N and two O atoms. This distance is considerably longer in the singlet structure than in the triplet one (2.40 vs. 2.27 Å), in agreement with a square-planar favoured coordination for a Cu(III)-d^8 centre. Conversely, all the other Cu-N and Cu-O bond distances are shorter in the singlet species.

The characterization of the hydroxylation product **C** as a Cu(III) species contrasts with the description of a similar product in the Itoh's system as Cu(II) complex with a triplet ground state.[12c] Accurate calculation of the energy splitting between low-spin and high-spin states of copper compounds in different oxidation states is difficult due to its strong functional dependence.[25] All the energies reported herein have been obtained with the hybrid meta-GGA TPSSh functional supplemented with the Grimme's dispersion correction D3, with the extended basis set basis-II (BS2, see SI). This 10% exchange functional accurately reproduces the relative energies of spin states of first-row transition metal complexes and predicts the reactivity of Cu(III).[26] However, in order to be fully confident about the correct electronic ground state of intermediate **C**, we performed single point electronic energy calculations, using a set of functionals, on TPSSh/BS1 optimized geometries of **C-CSS** and **C-T** with a more extended basis-III (BS3, see SI). Furthermore, we have performed calculations with the highly correlated coupled cluster single and double excitations, and perturbatively estimated triple excitations, [CCSD(T)], within a domain-based local pair natural orbital (DLPNO) formulation, at the TPSSH-D3/BS1 optimized geometries of **C-CSS** and **C-T**. This approach has already been used as a benchmark to estimate singlet-triplet gaps in copper complexes.[27]

The hydroxylation reaction analysed in the precedent section implies computing three different oxidation states of copper (I, II, and III) and two different spin states (singlet and triplet). Table S1 (in SI) collects the relative energies of Cu(I) (**1** + O_2 triplet), Cu(II) (**C-T**) and Cu(III) (**C-CSS**) as well as the singlet-triplet Cu(II)/Cu(III) energy gap computed with the different methods. Most accurate DLPNO-CCSD(T) calculations agree with a Cu(III)-singlet character of intermediate **C**, which is about 20 kcal mol^{-1} more stable than the Cu(II)-triplet isomer and 40 kcal mol^{-1} below the reactants (**1** + O_2 triplet). Taking the DLPNO-CCSD(T) values as a reference, the data collected in Table S1 highlight the difficulties of DFT functionals to describe in a balanced way such situations. Anyway, and despite significant changes in the relative energies, DLPNO-CCSD(T) and all the functionals, with the exception of M11, agree in assigning a singlet ground state to **C**, between 5 and 20 kcal mol^{-1} more stable than the Cu(II) triplet isomer. Thus, it can be safely assumed that *the mononuclear species **C** resulting from the hydroxylation of **1** is a Cu(III)-alkoxy-hydroxyl intermediate*.

In the next section we will address how this intermediate evolves toward the final, experimentally characterized trinuclear complex **2a**.

*From intermediate **C** to **2a**: Comproportionation and role of Cu(0).*

As evidenced by the optimized structures of **1** and **C** (Fig. 2), the steric hindrance of the $Tp^{Ms}Cu$ core precludes its interaction with the Cu(III) intermediate ensuing reduction, as it happened in the Itoh's system:[12c] only a Cu(0) atom can approach efficiently toward that end. We have placed a Cu(0) atom in the vicinity of the oxygen atoms of **C** and optimized the bimetallic system in the doublet spin state. Optimization leads to the complex **C-Cu**, depicted in Fig. 5. According to spin density values (Fig. 5), a comproportionation reaction, in which the Cu(III)/Cu(0) centres become Cu(II)/Cu(I), occurs upon formation of the bimetallic species.

The spin density over the initial Cu(0) radical almost vanishes, and is transferred to the initial Cu(III) centre. Some spin density is also delocalized over the two oxygen atoms. The redox process results in a huge stabilization of the system: the bimetallic Cu(II)-Cu(I) complex lies 81.3 kcal mol^{-1} below the separated Cu(III) (**C)** and Cu(0) atom (ΔG_{THF}). Optimization of **C-Cu** in the quartet spin states gives one structure that is 42.3

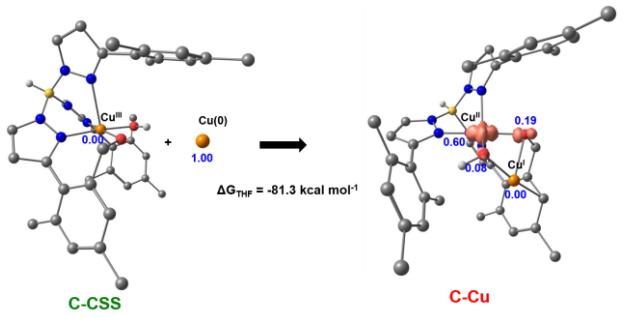

Fig. 5 Optimized structures of the $Tp^{Ms}Cu$ core **1** and intermediate C in Scheme 4 (left) and their space filling pictures (right). C-H bonded hydrogen atoms have been omitted in the optimized geometries.

kcal mol^{-1} above the doublet. Thus, the doublet is the ground state of **C-Cu**.

We have no experimental evidences for that bimetallic complex intermediate when employing **1-THF** or **1a,b** as reactants, all having 3-mesitylpyrazolyl groups. We reasoned that to block the incorporation of the third copper centre to the binuclear intermediate, a more sterically hindered ligand should be employed. Thus, we designed and synthetized the novel, bulkier Me-$Tp^{Me2\text{-}biphen}$ ligand with a biphenyl substituent at the pyrazolyl ring, increasing the steric hindrance of the ancillary ligand when coordinated at the copper centre in complex **4** (Scheme 5; see SI for characterization). This compound was reacted with O_2 following the above protocols. A very slow transformation took place, and after two weeks standing at room temperature, some crystalline material deposited. X-ray studies were performed with those crystals: although the quality of collected data for the new compound **5** precludes a complete structural description, its connectivity agrees with that depicted in Scheme 5. We believe that the formation of **5** demonstrate the participation of the dinuclear intermediate in the pathway leading to the trinuclear compounds described above. The low yield (ca. 13%) can be explained as the result of the presence of the Me-B bonded to boron and a more sterically protected copper centre, the decomposition route producing Cu(0) (probably colloidal copper) and free pyrazole being less favourable. Experiments carried out using **4**, O_2 and

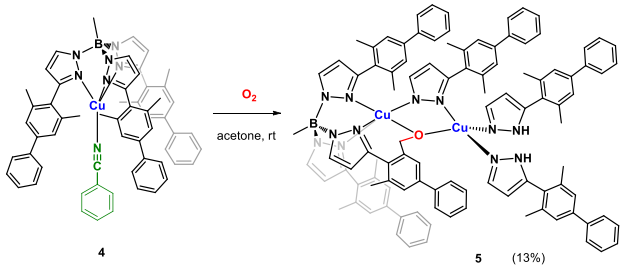

Scheme 5 Formation of dinuclear complex **5**.

added metallic copper and free pyrazole/pyrazolate were not successful. Refined structural details of the complex, as well as of its electronic structure, have been obtained by means of a DFT optimization (Fig. 6, see also SI).

In **5** both copper centres are not equivalent. One has a square-pyramidal arrangement of ligands, with five positions occupied by the three nitrogen atoms of the Me-$Tp^{Me2\text{-}biphen}$, the oxygen bonded to the activated methylene and a bridging pyrazolate ligand, coming from the partial decomposition of the starting complex. The spin density in this centre (0.58) agrees with a Cu(II) formulation. The second copper centre displays a

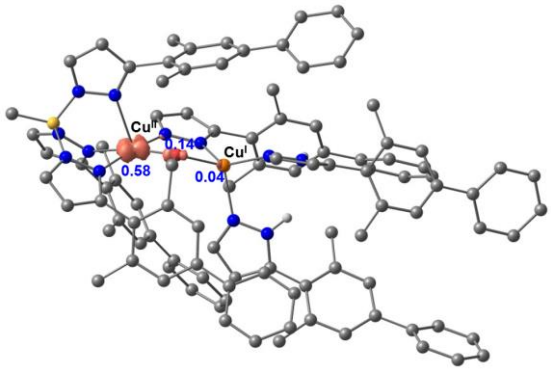

Fig. 6 Optimized structure of **5** showing its spin-density map (in orange) and Mulliken atomic spin populations (in blue).

tetrahedral coordination. It is bonded to four ligands: the bridging pyrazole, two pyrazoles and the oxygen. There is no spin density in this copper centre, as expected for a Cu(I) ion. From the optimized structure of **5** it is apparent that in this case further interaction with a third copper centre is avoided by the biphenyl groups. Thus, by using a very bulky ligand the

comproportionation process that yields the trimetallic complex has been stopped at the binuclear complex.

With the Tp^{Ms} ligand, the coordination of another mononuclear Cu(III) complex **C** to **C-Cu** is possible, forming in this way the trimetallic species **2a**. We have optimized the structure of **2a** both in the doublet (D) and quartet (Q) spin states. Computed structural parameters are very similar and agree with the X-ray determined ones (see SI). Analysis of the electronic structure of **2a** shows that its formation entails another internal redox process, in which the Cu(I) atom of **C-Cu** becomes formally a Cu(II) and the Cu(III) of the incoming **C** also becomes a Cu(II). Both the doublet and quartet optimized structures of **2a** have three equivalent copper (II) centres, with one unpaired electron each. The only difference between **2a**-D and **2a**-Q is that in **2a**-Q the three unpaired electrons have spin alpha, whereas in **2a**-D the unpaired electron of the central copper has a beta spin. Gibbs energy values at the TPSSh-D3/BS3 level of theory indicate that the **2a**-D is the most stable one, in contrast to the ferromagnetic behaviour observed experimentally. It should be noted, however, that the computed energy difference between **2a**-D and **2a**-Q is very small, (1.2 kcal mol^{-1}), and that packing effects in the solid may also influence the relative stability between these two almost degenerate spin states. There is a huge thermodynamic driving force directing the formation of the trimetallic copper(II) complex. The ΔG in THF for the formation of **2a** from two molecules of **C** and a copper atom is -148.4 kcal mol^{-1}. Accordingly, the copper(III)-alkoxy-hydroxyl intermediate is trapped as a trinuclear Cu(II) species.

Global mechanistic proposal

Based on experimental and computational data, Scheme 6 contains the global picture for the conversion of mononuclear copper(I) complexes bearing trispyrazolylborate-type ligands into trinuclear complexes **2a,b** after exposure to dioxygen atmosphere at room temperature. The interaction of the $Tp^{Ms}Cu$ core with O_2 yields the Cu(II) side-on superoxo **A** which evolves into a hydroperoxo intermediate **B** upon a HAT process. At this stage O-O cleavage takes place with concomitant formation of the alkoxy-hydroxy intermediate **C**, which reacts with Cu(0) en route to the dinuclear intermediate **D**. The latter contains two copper ions in +1 and +2 oxidation states, and serves as $1e^-$ source for another molecule of **C**, generating the trinuclear complex possessing three Cu(II) ions. It is of note that intermediate **C**, which could originate a Cu-oxyl and a hydroxyl radical, reacts in turn with Cu(0), precluding Fenton chemistry at variance with other reported systems. We cannot rule out the possible exchange of the OH ligand with adventitious water.

Conclusions

Dioxygen splitting and C-H bond oxidation with concomitant formation of alkoxy and hydroxyl groups are observed upon submitting complex $Tp^{Ms}Cu(L)$ (Tp^{Ms} = hydrotris(3-mesitylpyrazolyl)borate) to 1 atm of O_2 at room temperature. A copper(III)-alkoxy-hydroxy moiety has been trapped upon spontaneous reaction with metallic copper derived from decomposition of , leading to a trinuclear complex which has been characterized by X-ray studies. Computational studies have identified the crucial role of Cu(0) as a promotor of comproportionation reactions with Cu(III) species and support a dinuclear Cu(II)-Cu(I) species as intermediate on the pathway towards **2a**. These studies provide another view of C-H bond oxidation by copper centres under biological reaction conditions of pressure and temperature

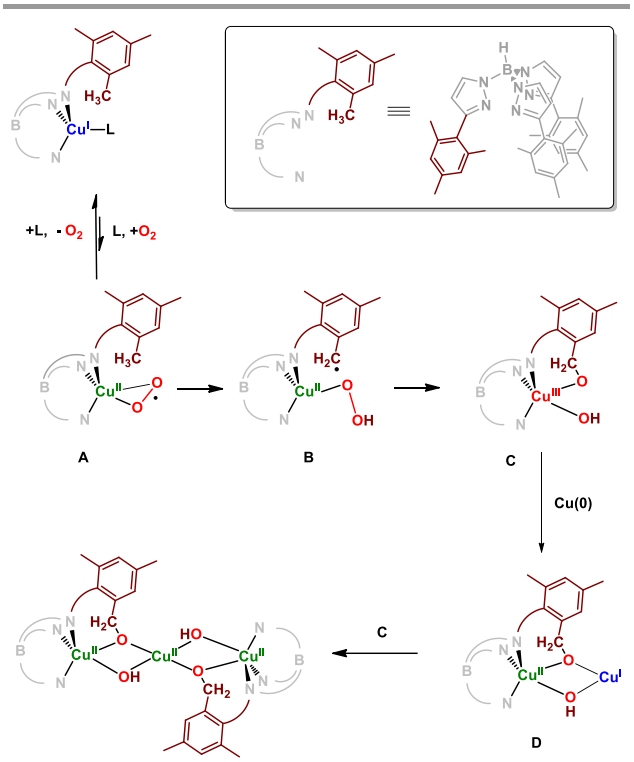

Scheme 6 The reaction pathway from mononuclear Cu^{I} complexes to the trinuclear Cu^{II} compounds involving Cu^{III} and Cu(0).

Conflicts of interest

There are no conflicts to declare.

Acknowledgements

Support for this work was provided by the MINECO (CTQ2017-82893-C2-1-R CTQ2017-87889-P and CTQ2017-89132-P) and P.O. FEDER 2014-2020, UHU-1260216. MA thanks Ministerio de Economía y Competitividad for an FPI predoctoral fellowship.

Notes and references

.

PAPER

1 (*a*) E. I. Solomon, D. E. Heppner, E. M. Johnston, J. W. Ginsbach, J. Cirera, M. Qayyum, M. T. Kieber-Emmons, C. H. Kjaergaard, R. G. Hadt and L. Tian, *Chem. Rev.* 2014, **114**, 3659–3853; (*b*) G. M. Yee, W. B. Tolman, *Transition Metal Complexes and the Activation of Dioxygen*. In *Sustaining Life on Planet Earth: Metalloenzymes Mastering Dioxygen and Other Chewy Gases* chapter 5, pp 131-204 (2014).

2 (*a*) J. P. Klinman, *Chem. Rev.* 1996, **96**, 2541–2562; (*b*) E. I. Solomon, U. M. Sundaram, T. E. Machonkin, *Chem. Rev.,* 1996, **96**, 2563–2606; (*c*) M. Fontecave, J.-L. Pierre, *Coord. Chem. Rev.,* 1998, **170**, 125–140.

3 (*a*) V. C. C. Wang, S. Maji, P. P.-Y. Chen, H.-K. Lee, S. S.-F. Yu, S. I. Chan, *Chem. Rev.,* 2017, **117**, 8574–8621; (*b*) T. J. Lawton, A. C. Rosenzweig, *Curr. Op. Chem. Biol.,* 2016, **35**, 142–149.

4 O. M. Ross, F. MacMillan, J. Wang, A. Nisthal, T. J. Lawton, B. D. Olafson, S. L. Mayo, A. Rosenzweig, B. Hoffman, *Science,* 2019, **364**, 566–570.

5 (*a*) C. E. Elwell, N. L. Gagnon, B. D. Neisen, D. Dhar, A. D. Spaeth, G. M. Yee, W. B. Tolman, *Chem. Rev.,* 2017, **117**, 2059–2107; (*b*) R. Tramell, K. Rajabimoghadam, I. Garcia-Bosch, *Chem. Rev.,* 2019, **119**, 2954–3031.

6 D. A. Quist, D. E. Diaz, J. L. Liu, K. D. Karlin, *J. Biol. Inorg. Chem.,* 2017, **22**, 253–288.

7 (*a*) K. Fujisawa, M. Tanaka, Y. Moro-Oka, N. A Kitajima, *J. Am. Chem. Soc.*, 1994, **116**, 12079–12080; (*b*) P. Chen, D. E. Root, C. Campochiaro, K. Fujisawa, E. I. Solomon, *J. Am. Chem. Soc.,* 2003, **125**, 466–474; (*c*) C. Würtele, E. Gaoutchenova, K. Harms, M. C.; Holthausen, J. Sundermeyer, S. Schindler, *Angew. Chem., Int. Ed*., 2006, **45**, 3867–3869; (*d*) D. J. E. Spencer, N. W. Aboelella, A. M. Reynolds, P. L. Holland, W. B. Tolman, *J. Am. Chem. Soc.,* 2002, **124**, 2108–2109. (e) K. Fujisawa, T. Ono, Y. Ishikawa, N. Amir, Y. Miyashita, K.-I. Okamoto, N. Lenhert, *Inorg. Chem*. 2006, **45**, 1698-1713.

8 J. J. Liu, D. E. Diaz, D. A. Quist, K. D. Karlin, *Isr. J. Chem*., 2016, ***56***, 738 – 755.

9 (*a*) D. Maiti, D.-H. Lee, K. Gaoutchenova, C. Würtele, M. C. Holthausen, A. A. N. Sarjeant, J. Sundermeyer, S. Schindler, K. D. Karlin, *Angew. Chem. Int. Ed.,* 2008, **47**, 82–85; (*b*) M. Bhadra, J. Y. C. Lee, R. E. Cowley, S. Kim, M. A. Siegler, E. I. Solomon, K. D. Karlin, *J. Am. Chem. Soc.,* 2018, **140**, 9042–9045; (*c*) D. E. Diaz, D. A. Quist, A. E. Herzog, A. W. Schaefer, I. Kipouros, M. Bhadra, E. I. Solomon, K. D. Karlin, *Angew. Chem. Int. Ed.,* 2019, **58**, 17572–17576.

10 (*a*) Y. Y. See, A. T. Herrmann, Y. Aihara, P. S. Baran, *J. Am. Chem. Soc.,* 2015, **137**, 13776–13779; (*b*) R. Trammell, Y. Y. See, A. T. Herrmann, N. Xie, D. E. Díaz, M. A. Siegler, P. S. Baran, I. Garcia-Bosch, *J. Org. Chem.,* 2017, **82**, 7887–7904.

11 S. Kim, J. W. Ginsbach, J. Y. Lee, R. L. Peterson, J. J. Liu, M. A. Siegler, A. A. Sarjeant, E. I. Solomon, K. D. Karlin, *J. Am. Chem. Soc.,* 2015, **137**, 2867–2874.

12 (*a*) S. Itoh, *Acc. Chem. Res.,* 2015, **48**, 2066–2074; (*b*) T. Tano, Y. Okubo, A. Kunishita, M. Kubo, H. Sugimoto, N. Fujieda, T. Ogura, S. Itoh, *Inorg. Chem.,* 2013, **52**, 10431–10437; (*c*) A. Kunishita, M. Z. Ertem, Y. Okubo, T. Tano, H. Sugimoto, K. Ohkubo, N. Fujieda, S. Fukuzumi, C. J. Cramer, S. Itoh, *Inorg. Chem.*, 2012, **51**, 9465–9480; (*d*) A. Kunishita, M. Kubo, H. Sugimoto, T. Ogura, K. Sato, T. Takui, S. Itoh, *J. Am. Chem. Soc.*, 2009, **131**, 2788–2789.

13 J. L. Schneider, S. M. Carrier, C. E. Ruggiero, V. G. Young Jr., W. B. Tolman, *J. Am. Chem. Soc.* 1998, **120**, 11408 – 11418.

14 CCDC 1998194 (**1a**), 1998192 (**1b**), 1998369 (**2a**), 1998208 (**2b**), 1998370 (**3a**) 1998191 (**3b**), contain the supplementary crystallographic data for this paper. These data can be obtained free of charge from The Cambridge Crystallographic Data Centre

15 K. D. Karlin, Y. Gultneh, J. P. Hutchinson, *J. Am. Chem. Soc.* 1982, **104**, 5240-5242.

16 (a) E. A. Lewis, W. B. Tolman, *Chem. Rev.* 2004, **104**, 1047-1076; (b) S. Mahapatra, J. A. Halfen, E. C. Wilkinson, L. Que, Jr., W. B. Tolman, *J. Am. Chem. Soc.* 1994, **116**, 9785-9786.

17 M. Ruf, C. G. Pierpont, *Angew. Chem. Int. Ed.,* 1998, **37**, 1736–1739.

18 A. Bondi, *J. Phys. Chem.,* 1964, **68,** 441–451.

19 A. Ozarowski, C. J. Calzado, R. J. Sharma, S. Kumar, J. Jezierska, C. Angeli, F. Spizzo, V. Ferretti, *Inorg. Chem.,* 2015, **54**, 11916–11934.

20 J. L. Kisko, T. Hascall, G. Parkin, *J. Am. Chem. Soc.* 1998, **120**, 10561-10562.

21 R. Dias, X. Wang, *Polyhedron* 2004, **23**, 2533-2536.

22 M. Smith, *Organic Synthesis*, 4th ed. Academic Press, 2016.

23 M. A. Mairena, J. Urbano, J. Carbajo, J. J. Maraver, E. Álvarez, M. M. Díaz-Requejo, P. J. Pérez, *Inorg. Chem*. 2007, **46**, 7428-7435.

24 Y.-R. Luo, *Comprehensive Handbook of Chemical Bond Energies*, CRC Press, Boca Ratón, 2007.
25 (*a*) B. F. Gherman, C. J. Cramer, *Coord. Chem. Rev.,* 2009, **253**, 723–753; (*b*) B. Dereli, M. A. Ortuño, C. J. Cramer, *ChemPhysChem,* 2018, **19**, 959–966.
26 J. Cirera, M. Via-Nadal, E. Ruiz, *Organometallics,* 2015, **34**, 1294–1300.
27 M. Mandal, C. E. Elwell, C. J. Bouchey, T. J. Zerk, W. B. Tolman, C. J. Cramer, *J. Am. Chem. Soc.,* 2019, **141**, 17236–17244.

